

A	TCR-pHLA interface BSA (\AA^2 , % total)							
	pHLA		Peptide		HLA helix- α 1		HLA helix- α 2	
NYE_S1 TCR α chain	434	30.3	272	46.8	79	13.2	82	33.4
NYE_S1 TCR β chain	997	69.7	309	53.2	523	86.8	164	66.6
NYE_S2 TCR α chain	776	47.6	343	61.8	191	26.2	242	70.0
NYE_S2 TCR β chain	855	52.4	212	38.2	540	73.8	104	30.0
NYE_S3 TCR α chain	337	31.0	156	31.9	3	0.9	178	65.1
NYE_S3 TCR β chain	748	69.0	332	68.1	321	99.1	95	34.9
1G4 TCR α chain	788	46.7	352	53.1	160	25.6	276	69.3
1G4 TCR β chain	898	53.3	311	46.9	465	74.4	122	30.7

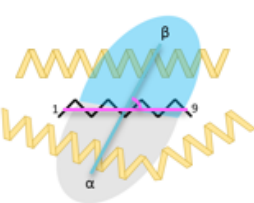
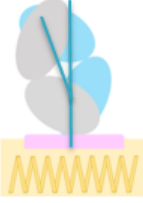
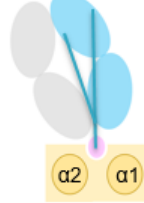
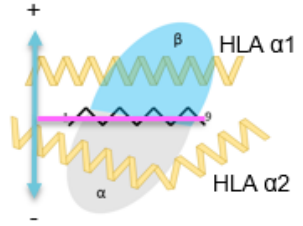
B	TCR docking geometry			
	TCR/HLA cross ($^\circ$)	TCR/HLA tilt ($^\circ$)	TCR/HLA roll ($^\circ$)	TCR shift towards HLA helix- α 1 (\AA)
				
1G4	70.0	10.5	-15.3	3.85
NYE_S1	70.4	13.4	-22.2	4.36
NYE_S2	74.0	14.1	-24.9	6.34
NYE_S3	64.7	-3.2	-10.3	0.28

Table S1. TCR-pHLA interface BSA and docking geometry analysis. **A)** Characterisation of NYE_S1, NYE_S2, NYE_S3 and 1G4 TCR α and β chain contributions to the TCR-pHLA interface measured by buried surface area (BSA). **B)** Characterisation of NYE_S1, NYE_S2, NYE_S3 and 1G4 TCR docking geometries on pHLA. For NYE_S1 and NYE_S3 TCR-pHLA structures, which contain more than one TCR-pHLA copy in the ASU, chains A-E (copy 1) was used for this analysis. 1G4; TCR-pHLA NY-ESO-1₁₅₇₋₁₆₅(9V) (PDB ID 2BNQ).

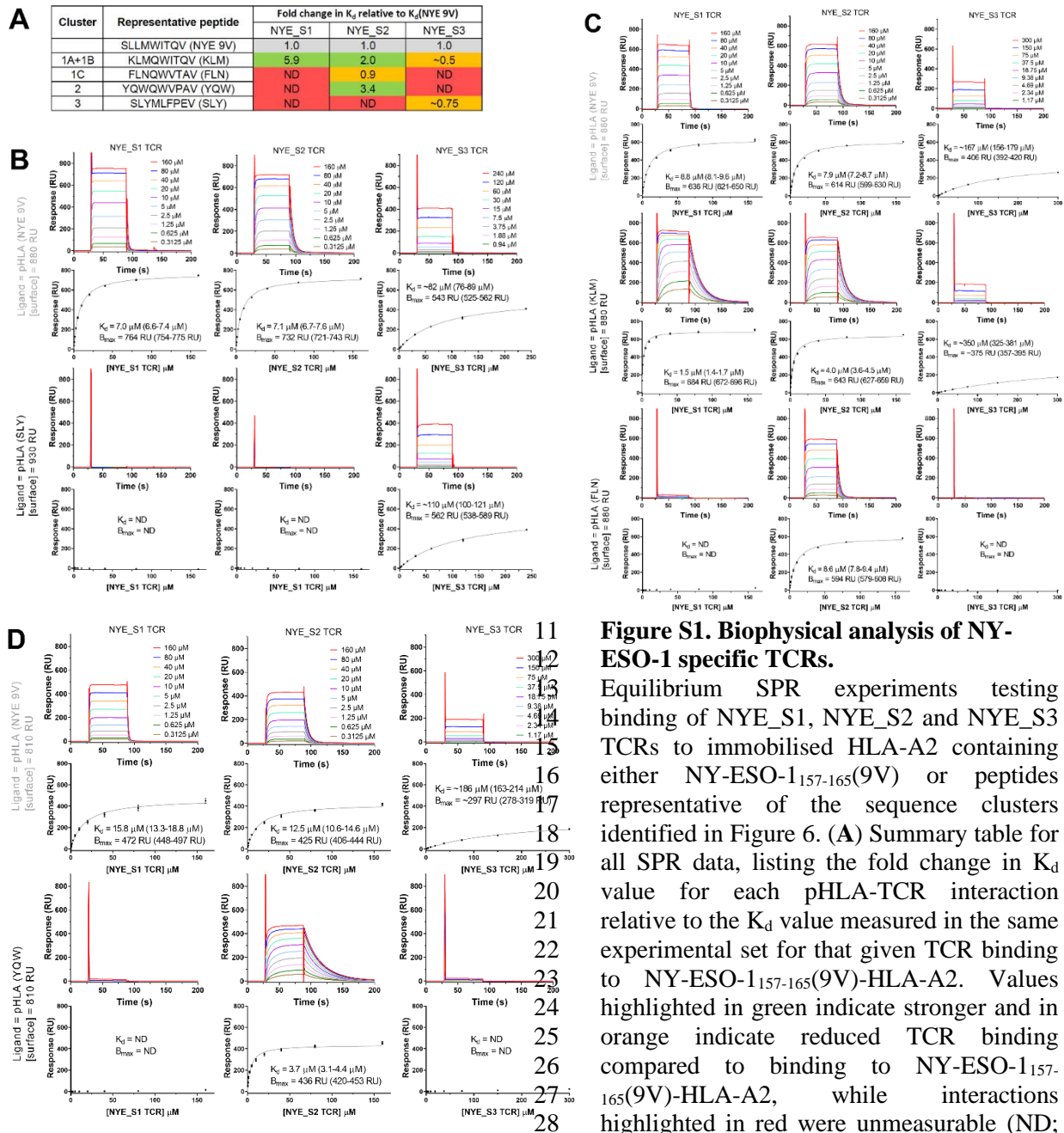


Figure S1. Biophysical analysis of NY-ESO-1 specific TCRs.

Equilibrium SPR experiments testing binding of NYE_S1, NYE_S2 and NYE_S3 TCRs to immobilised HLA-A2 containing either NY-ESO-1₁₅₇₋₁₆₅(9V) or peptides representative of the sequence clusters identified in Figure 6. (A) Summary table for all SPR data, listing the fold change in K_d value for each pHLA-TCR interaction relative to the K_d value measured in the same experimental set for that given TCR binding to NY-ESO-1₁₅₇₋₁₆₅(9V)-HLA-A2. Values highlighted in green indicate stronger and in orange indicate reduced TCR binding compared to binding to NY-ESO-1₁₅₇₋₁₆₅(9V)-HLA-A2, while interactions highlighted in red were unmeasurable (ND; not determined). Supporting data for all SPR experiments testing binding of NYE_S1, NYE_S2 and NYE_S3 TCRs to immobilised: (B) NY-ESO-1₁₅₇₋₁₆₅(9V)-HLA-A2 and SLYMLFPEV-HLA-A2, (C) NY-ESO-1₁₅₇₋₁₆₅(9V)-HLA-A2, KLMQWITQV-HLA-A2 and FLNQWVTAV-HLA-A2, (D) NY-ESO-1₁₅₇₋₁₆₅(9V)-HLA-A2 and YQWQWPAV-HLA-A2. All experiments were performed at 25°C in triplicate; a representative set of sensograms (top panel) and a binding curve fitted to all repeats (bottom panel) is shown for each interaction. Error bars for each binding curve data point correspond to standard deviation. Mean K_d and B_{max} values estimated from the binding curves are stated, together with 95 % confidence interval in brackets (lower-upper limit). Legends provided for each TCR in the top sensogram apply to all other sensograms for that TCR within the same panel. No significant response was measured when testing the three TCRs against >14 irrelevant peptide HLA-A2 complexes (data not shown).

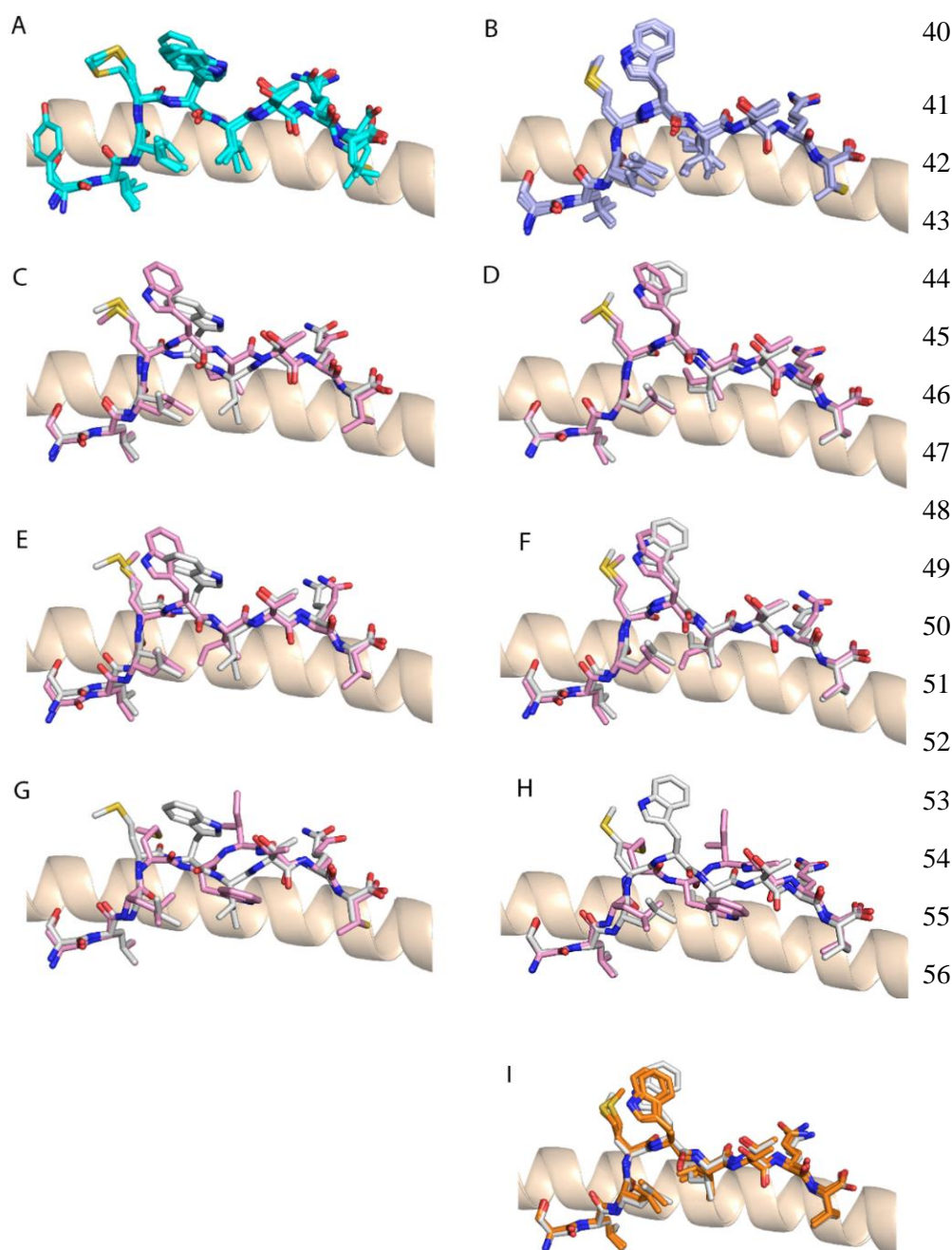
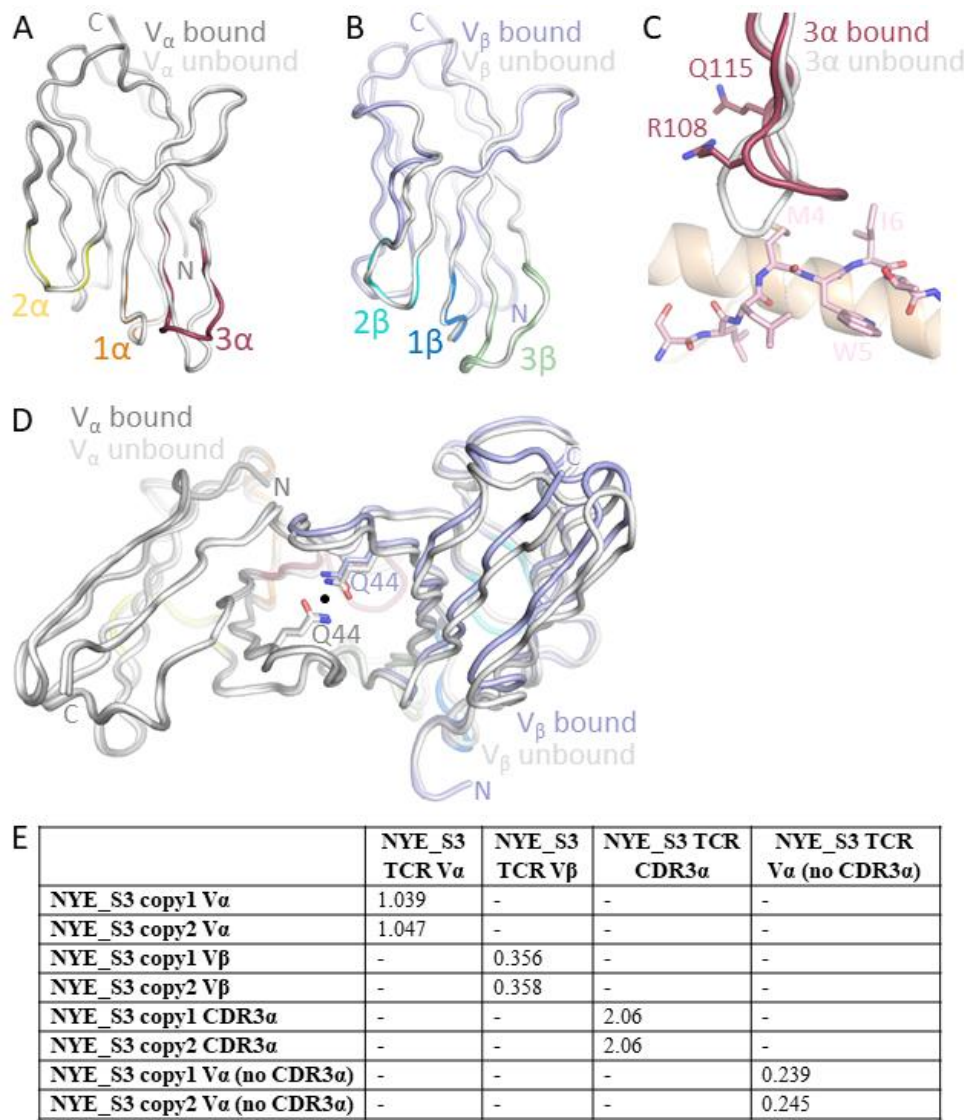


Figure S2. Comparison of NY-ESO-1₁₅₇₋₁₆₅ peptide conformations observed in crystal structures containing NY-ESO-1₁₅₇₋₁₆₅-HLA-A2. (A) NY-ESO-1₁₅₇₋₁₆₅ conformations in apo pHLA structures: SLLMWITQC peptide (PDB ID 1S9W), SLLMWITQY (1S9X, 1S9Y), SLLMWITQL (3KLA), YLLMWITQV (4L29). Alignment on 1S9W chain A residues 57-84 (HLA helix-α1). (B) TCR bound NY-ESO-1₁₅₇₋₁₆₅ conformations: wildtype (PDB ID 2BNQ, SLLMWITQV peptide) and affinity enhanced (PDB ID 2BNR, 2F53, 2F54, 2P5E, 2P5W, 2PYE, all SLLMWITQC) 1G4 TCR-pHLA structures. Alignment on 2BNQ chain A residues 57-84 (HLA helix-α1). (C, E, G) NY-ESO-1₁₅₇₋₁₆₅ conformations TCR-pHLA structures (SLLMWITQV peptides coloured pink) compared to apo pHLA structure 1S9W (SLLMWITQC peptide grey) for NYE_S1, RMSD 0.955 Å, NYE_S2, RMSD 0.826 Å and NYE_S3, RMSD 1.36 Å over 9Cα atoms. Alignment to 1S9W chain A residues 57-84 (HLA helix-α1). (D, F, H) NY-ESO-1₁₅₇₋₁₆₅ conformation in 1G4 TCR-pHLA structure 2BNQ (SLLMWITQV peptide grey) compared to TCR-pHLA structures (SLLMWITQV peptides coloured pink) for NYE_S1, 0.262 Å 9Cα, NYE_S2, 0.261 Å 9 Cα and NYE_S3. Alignment to 2BNQ chain A residues 57-84 (HLA helix-α1). (I) ScFv bound NY-ESO-1₁₅₇₋₁₆₅ conformations (3M4E5, PDB ID 3GJF and 3M4F4, 3HAE, SLLMWITQV peptides coloured orange) compared to wildtype 1G4 TCR-pHLA structure (2BNQ, SLLMWITQV peptide grey). For all panels, peptides are shown in stick representation and the HLA helix-α1 as wheat coloured ribbons.

78



79

Figure S3. Structural comparison of NY-ESO-1₁₅₇₋₁₆₅-HLA-A2 bound versus unbound NYE_S3 TCR. (A) Unbound TCR Vα domain aligned to bound TCR Vα from TCR-pHLA copy 1 in S3 crystal structure (alignment based on Cα positions for residues 8-128). (B) Unbound TCR Vβ domain aligned to bound TCR Vβ from TCR-pHLA copy 1 in NYE_S3 crystal structure (alignment based on Cα positions for residues 8-128). (C) Unbound TCR Vα domain aligned onto TCR-pHLA copy 1 in S3 crystal structure (alignment as in (A)). Peptide, pink sticks; HLA helix-α1, wheat ribbon. (D) Unbound TCR Vα domain aligned to bound TCR Vα from TCR-pHLA copy 1 in NYE_S3 crystal structure (alignment as in (A)). View shown looking down the symmetry axis of the TCR (indicated by the black circle), through the hydrogen bonded TCRα Q44-TCRβ Q44 sidechains towards pHLA. N, Vα or Vβ N-terminus; C, Vα or Vβ C-terminus. (E) RMSD (Å) between TCRs in the two TCR-pHLA copies versus one unbound TCR copy in ASU for S3 (comparing Cα positions for either Vα residues 8-128, Vβ 3-128, CDR3α 105-117 or Vα (no CDR3α) 8-105 and 117-128).